

# Optical Measurement of Transient Plasma Impact on Corner Separation in $M=4.5$ Airflow

Alec Houpt<sup>1</sup>, Stanislav Gordeyev<sup>2</sup>, Thomas Juliano<sup>3</sup>, and Sergey Leonov<sup>4</sup>

*FlowPAC Institute, AME Dept, University of Notre Dame, Notre Dame, IN,*

**The objective of this work is to perform a feasibility study on the steering effect of a weakly ionized transient plasma on the corner separation zone of a compression surface with a hypersonic boundary layer. The optical measurements, using a high-speed Shack-Hartmann sensor, have been successfully performed to quantify a characteristic frequency of flow perturbations at different locations in the flowfield and the plasma impact on the spectra of disturbances in the boundary layer and in the separation bubble. It was shown that the near-surface plasma generation at a frequency of repetition higher than a dominant natural frequency of perturbations in the boundary layer (the first mode  $F_1$ ),  $f = 100 \text{ kHz} > F_1 \approx 65 \text{ kHz}$ , lead to a significant intensification of the amplitude of the high-frequency disturbances in the range of  $A/A_0 = 2 - 8$ . The plasma effect was negligible or insignificant at excitation frequencies,  $f = 50 \text{ kHz}$ , below  $F_1$ .**

## I. Introduction

Intensive studies of the physical processes of hypersonic boundary-layer tripping have been motivated by the needs of scramjet systems for air-breathing vehicles. For airframe-integrated scramjet engines, the forebody ahead of the inlet is designed to process and pre-condition the flow that will be ingested by the air inlet. Turbulent flow is desirable at the entrance to the inlet to mitigate flow separations on compression ramps and prevent air inlet unstarts [1-2]. However, natural transition typically does not occur on small-scale systems flying at high altitude (low Re number), thereby requiring boundary layer trip devices to ensure a turbulent boundary layer at the inlet. This issue motivated development of various boundary layer trip methods to promote turbulent flow in order to properly scale the engine flight test results to future full-scale vehicles. It was suggested that the most effective tripping mechanism requires the formation of streamwise vorticity within the boundary layer [3-6]. Typically, obstacles, moving elements, or non-steady gas jets are used to promote transition on the forebody. Recently, a thermal type of BL management was considered to be feasible [7].

The non-thermal trips previously mentioned produce stationary forcing of the boundary-layer flow. They enhance and/or trigger instability mechanisms. However, they do not generate unstable disturbances. The latter are produced by the freestream noise or the incoming boundary layer. It is reasonable to assume that unsteady forcing, which generates disturbances of required length-scale and frequency, may be much more effective. Such an unsteady forcing can be produced by synthetic jets and/or plasma actuators.

The primary mechanisms of plasma flow control include thermal (heating of the gas), electro-hydro-dynamic (EHD), and magneto-hydro-dynamic (MHD) interactions. EHD and MHD interactions induce bulk fluid motions via collisional momentum transfer from charged species accelerated in the plasma by Coulomb and Lorentz forces,

---

<sup>1</sup> Graduate Student, Department of Mechanical and Aerospace Engineering, Hessert Laboratory for Aerospace Research, Notre Dame, IN 46556.

<sup>2</sup> Research Associate Professor, Department of Mechanical and Aerospace Engineering, Hessert Laboratory for Aerospace Research, Notre Dame, IN 46556, AIAA Associate Fellow.

<sup>3</sup> Assistant Professor, Department of Mechanical and Aerospace Engineering, Hessert Laboratory for Aerospace Research, Notre Dame, IN 46556, AIAA Senior Member.

<sup>4</sup> Research Professor, Department of Mechanical and Aerospace Engineering, Hessert Laboratory for Aerospace Research, Notre Dame, IN 46556, AIAA Associate Fellow.

respectively. Heating of the flow is produced by Joule heating in an electric discharge plasma and in the plasma generated by laser breakdown.

Plasmas generated for flow actuation have been extensively studied over the last decade [8-13, and references therein]. Most of the existing research is related to Surface Dielectric Barrier Discharge (SDBD) plasma actuators that are typically driven by AC waveforms or by repetitive nanosecond duration pulses, with frequencies / pulse repetition rates ranging from a few kHz to a few tens of kHz. Determining whether the SDBD-actuator effect on the flow under compressible conditions is caused by an EHD body force or by localized Joule heating remains an open question. In the case of fast Joule heating on the order of a nanosecond time scale the generation of a compression wave was detected. In spite of these detailed studies, it was not directly evident that compression waves generated by heating on a sub-acoustic time scale are indeed the dominant factor in the boundary layer tripping or generation of the coherent flow structures. Another issue is a low level of power deposition for the SDBD-based system that makes it unlikely to be used in a high-speed environment. The fundamental limitation on the use of EHD flow control is the necessity to generate a significant ion density in the space charge region of the electric discharge (i.e. cathode sheath of the glow discharge). Thus the use of EHD for high-speed flow control (with flow velocities of a few hundred m/s) does not appear feasible.

Similarly, for the MHD flow control the fundamental limitation is the requirement to sustain significant flow conductivity, except for high-temperature hypersonic reentry flows. For example, in a hypersonic flow with a velocity of  $U_\infty \sim 1000$  m/s and conductivity of  $\sigma \sim 1.0$  mho/m, the MHD effect can be significant only at very low densities,  $\rho \sim 10^{-3}$  kg/cm<sup>3</sup> ( $p \sim 1$  mBar). Finally, sustaining higher conductivity using non-equilibrium plasmas is limited by ionization instabilities and requires a prohibitively-high plasma power budget.

Another group of plasma-related studies is focused on high-speed applications [14-20]. Various methods of plasma generation, including DC, AC, RF, microwave, arc, corona, and spark electric discharges, as well as laser-induced breakdown, have been used to modify both subsonic and supersonic flow fields. Engineering applications of plasma actuators mainly focus on viscous drag reduction and the control of the boundary layer separation in low-speed flows, dynamic stall control, boundary-layer transition control as well as shock wave modification and wave drag reduction in supersonic and hypersonic flows. Previous research on purely thermal flow control includes energy addition using bulk heating of the flow by plasma. However, bulk heating of the flow in a high-speed flow field requires a very high plasma power budget (comparable with the flow enthalpy).

It is well known that intense, localized, rapid heating produced by plasmas in high-current pulsed electric discharges (similar to pulsed optical discharges) may produce strong shock waves, which can considerably modify supersonic flows over blunt bodies. The energy transfer from the electric field to the electrons is almost instantaneous while the transfer of energy from the electrons to the gas molecules goes through a series of processes: vibrational excitation, dissociation, and ionization followed by relaxation. The relaxation and recombination times are slow compared to the gas dynamic time of hypersonic flows. Basically, rapid near-adiabatic heating results in an abrupt pressure jump in the current filament. This suggests that rapidly heated regions located near aerodynamic surfaces could be used to force various instabilities in shear layers and jets. The key benefit of localized plasma actuators, compared to mechanical and acoustic actuators, is that they uniquely combine a wide range of operation frequencies with large forcing amplitude. Multiple plasma actuators can be independently controlled by varying the repetition rate, duty cycle, and the phase, making it possible to trigger and amplify specific flow instabilities. As a result, significant flow field changes can be produced at a relatively small energy cost to operate plasma actuators.

The objective of this work is to perform a feasibility study on the steering effect of a weakly ionized transient plasma on the corner separation zone on a compression surface of a hypersonic boundary layer. Specific tasks of current experiments included:

- Design of the plasma generator feasible to produce a pointwise, near-surface plasma at frequencies of 100-200 kHz in low pressure, high-speed flow;
- experimental study of the structure and dynamics of the gas pressure/density disturbances produced by the generation of transient plasma;
- experimental demonstration of the BL receptivity to plasma-based gas perturbations in hypersonic flow.

## II. Experimental Facility Description

The diagram of the test arrangement is shown in Fig. 1. The experiments were performed in the high-enthalpy facility ACT-1 at the University of Notre Dame under the following test parameters: Mach number  $M = 4.5$  (at nozzle exit); Reynolds number  $Re_L = 10^7$  (m<sup>-1</sup>); stagnation pressure  $P_0 = 0.8$  Bar; stagnation temperature  $T_0 = 300$  K and 1800 K; flow enthalpy from  $h \cdot \dot{m} \approx 10$  kW (cold flow) to 50 kW (hot flow). The model has length  $L = 229$  mm,

width  $W = 102 \text{ mm}$ , and thickness  $H = 19 \text{ mm}$ . It consists of a base plate with a sharp leading edge  $\alpha = 15^\circ$ . The compression ramp is formed with a second plate of equal thickness and a ramp angle  $\alpha = 20^\circ$ . The model is equipped with a ceramic insertion where multiple plasma generators are arranged in the spanwise-direction upstream of the ramp, as it is shown schematically in Fig. 1.

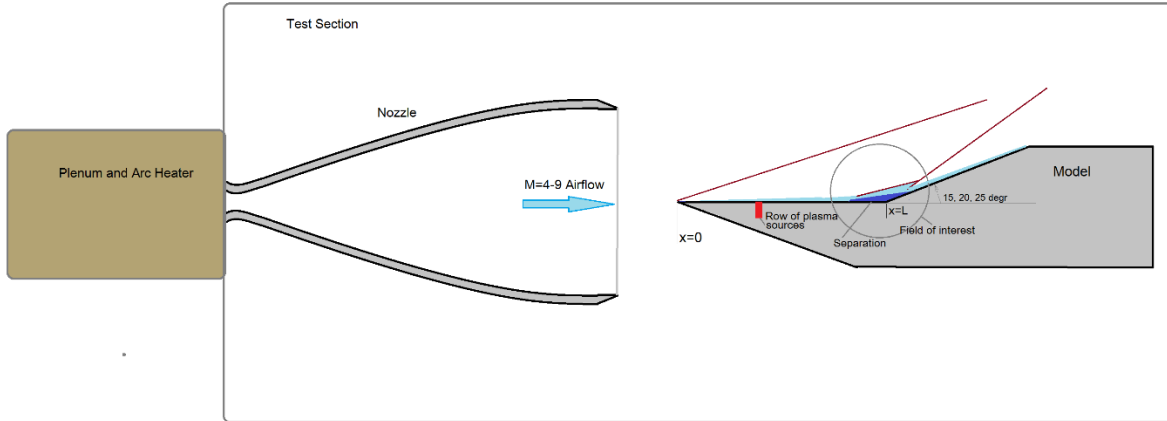


Fig. 1. Experimental arrangement.

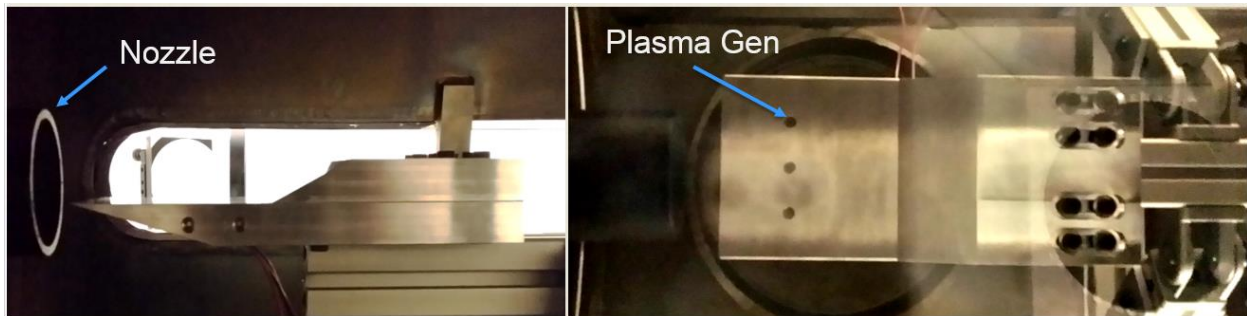


Fig. 2. Photo of the model in test section of ACT-1 facility at the University of Notre Dame.  $M = 4.5$  nozzle exit is visible on left side. Three plasma generators are indicated on the right image.

The ramp angle could be varied in a range  $\beta = 15 - 25^\circ$  to possess a flow pattern with or without the corner separation zone. In the current test the  $\beta = 20^\circ$  plate was applied. Photos of the experimental model are shown in Fig. 2. The test duration was  $t < 1 \text{ sec}$  including the arc operation (in the hot regime) for  $0.3 \text{ sec}$  and the plasma operation for  $0.1 \text{ sec}$  within the flow. All experimental data has been recorded with a baseline flow, with the plasma switched on, and after the plasma was switched off (baseline flow). This sequence allows verifying that there is no change of flow parameters during the operation.

Instrumentation and data includes: flow perturbation measurements made by a high-speed wavefront sensor (see below); schlieren visualization; fast cam imaging; and electrical measurements of the discharge parameters. Based on data in [21], the dominant instability on this model for these conditions is expected to be first-mode waves with a peak frequency of  $77 \text{ kHz}$ .

Three test series were performed:

- test 1: single plasma pulse generation in a stagnant air;
- test 2: single plasma pulse in flow;
- test 3: pulse periodic operation of plasma in the flow.

### III. Approach for Plasma Actuator Design.

Existing data [21-22] suggests that the most effective frequency of artificial disturbances for tripping the boundary layer at  $M = 5$  is  $f = 100 - 200 \text{ kHz}$ . For a proper optimization of the system the frequency of plasma operation has to be adjustable over a wide range. Taking into account the data on passive tripping, the geometry of the plasma array

may be specified as follows: one line in the spanwise direction with the distance between the individual electrode systems of  $d = 5 - 25 \text{ mm}$ . The averaged electrical power of each actuator should be in the range of  $P = 100 - 500 \text{ W}$  based on the local instant gas temperature elevation  $\Delta T \approx 10^2 - 10^3 \text{ K}$ . The duration of each plasma pulse should be  $\tau < 5 \mu\text{s}$  to produce the pointwise disturbances.

Note that a low level of gas density in a hypersonic boundary layer flow may cause a serious problem. It is well known that an electrical discharge changes its properties dramatically in low gas densities, striving to become a glow discharge where the power density becomes too low for the fast heating. Preliminary tests and previous literature indicate that it is possible to generate filamentary plasma at the molecular concentration of  $n > 2 \times 10^{17} \text{ cm}^3$  using a simple two-electrode scheme. For lower concentrations, a more complex design of the discharge system is required and, to the authors' knowledge, there are no open publications related to this subject. A proper configuration should be designed in accordance with the following criteria:

- Adequate plasma localization
- High enough instant power release
- Presence of shock disturbances
- Sufficiently high frequency of repetition
- Analysis of possible penalties

The scheme presented in Fig. 3 has been referred to as a shallow cavity discharge, or "SCD". The SCD actuator is flush mounted, with a size of a few millimeters and can be installed on the metallic surface of the model. It can be characterized by a proper discharge geometry, reasonably low applied voltage, and a high enough level of the disturbances excited. Typical records of the electric parameters in  $M=4.5$  flow are shown in Fig. 4 for two frequencies of repetition: 10 kHz and 50 kHz. The pulse energy and average power were calculated based on this data. The discharge parameters are as follows:

Frequency of repetitions	single pulse (tests 1 and 2); and $f = 10 - 100 \text{ kHz}$ (test 3)
Pulse duration	$t = 3 \mu\text{s}$
Voltage	$U < 2 \text{ kV}$
Pulse energy	$E = 1.2-1.7 \text{ mJ/unit}$
Average power	$W_{\text{av}} < 500 \text{ W}$

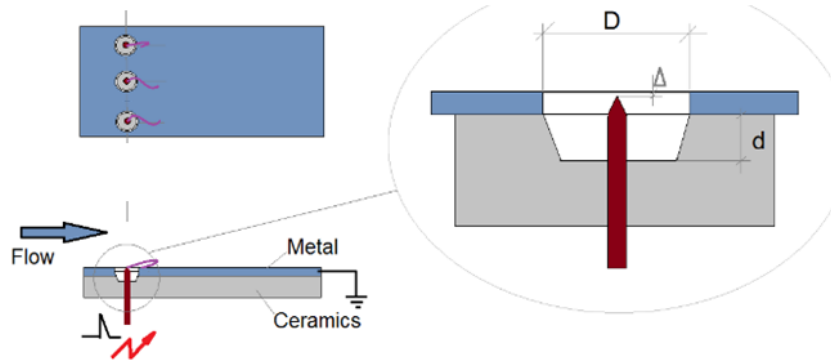


Fig. 3. Principal schematic of plasma BL actuator based on Shallow Cavity Discharge.

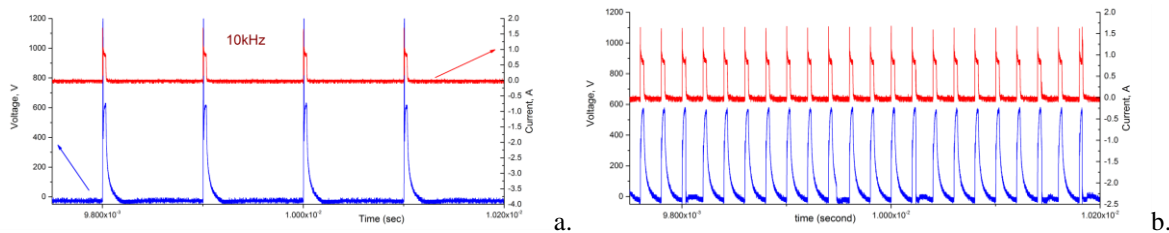


Fig. 4. Voltage –current time series of the SCD operation at  $f=10\text{kHz}$  (a) and  $f=50\text{kHz}$ .

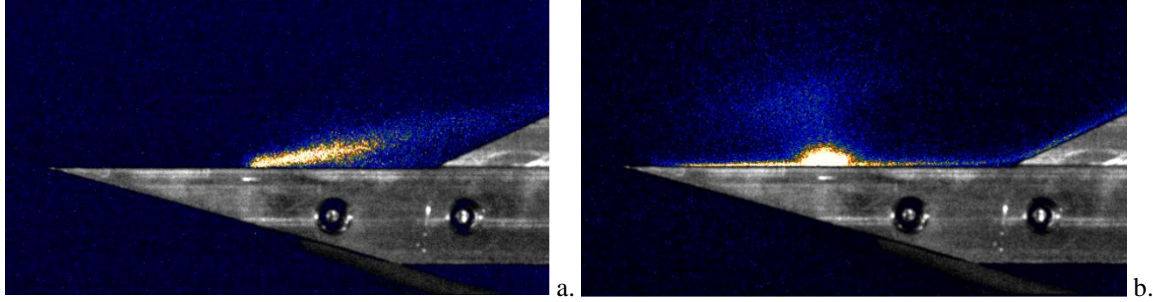


Fig. 5. Major operational modes of the SCD in  $M = 4.5$ ,  $P = 4$  mBar flow. a – plasma mini-jet; b – cathode sheath pattern. Exposure  $1\mu\text{s}$ , delay time  $3\mu\text{s}$  (within the electric pulse).

The high-speed camera observation shows that the discharge can operate in two different modes: plasma mini-jets; and a plane-wise pattern, as they are presented in Fig. 5. At  $f = 50 - 100$  kHz the discharge works in the first mode: push-pull plasma mini-jet. This mode was typically realized in this test. The second operation works in the second mode: cathode sheath pattern, where a rather thin layer of plasma covers most of the model surface. The cathode sheath is the place where a major part of the electric power is released [23]. Some features are not clear at the moment. This mode needs to be studied additionally to figure out a non-uniform pattern of the power release. A benefit of this mode could be in that the plasma localizes in the boundary layer.

#### IV. Aero-Optical Measurements

Aero-optical diagnostic measurements were performed using a high-speed Shack-Hartmann Wavefront Sensor [24]; a schematic of the experimental setup is shown in Fig. 6. The laser beam was expanded to a 50mm diameter collimated beam and passed along the spanwise direction over the corner region of the model mounted in the test section. The spanwise beam propagation was chosen for two reasons. First, the flow is expected to be primarily spanwise-uniform. Second, as the beam traverses the 4 inch long region of the flow aero-optical distortions become stronger, improving the signal-to-noise ratio [25]. After exiting the test section, the beam is reflected off the return mirror, which sends the beam along exactly the same path from which it came. This so-called double-path setup further amplifies the aero-optical signal by a factor of two, as the beam traverses through the flow of interest twice, and also simplifies the optical setup. The returning beam is split off using a cube beam splitter, sent through a contracting telescope which reduces the beam size to 12mm in diameter and goes into a high-speed digital camera, Phantom v1610. The camera had a 38 mm focal length, 70 x 60 lenslet, 0.3 mm pitch array attached to it. After passing through the lenslet array, the beam was split into subaperture beams and focused on the camera sensor, creating a series of dots. To achieve the high sampling rate, only a small, 128x64-pixel portion of the image, shown in Fig. 7, was sampled at 531,645 Hz for 4 seconds. This image size corresponds to a 15x7 mm measurement region over the model, with 1.2 mm spacing between dots.

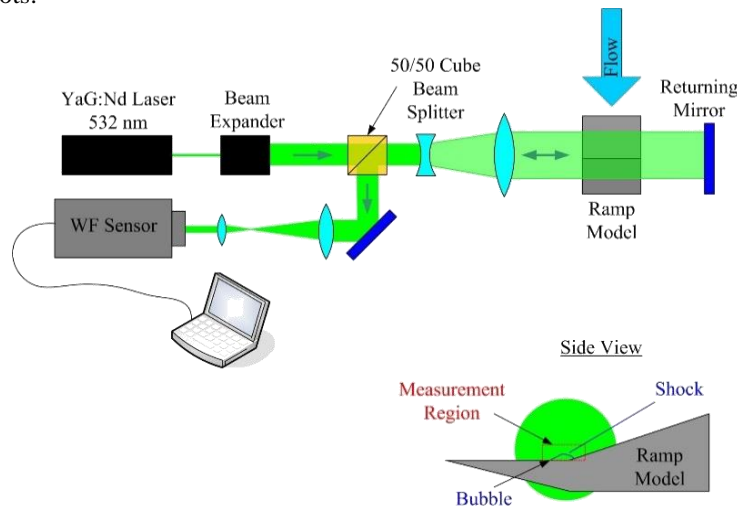


Fig. 6. Schematic of optical set-up.

A temporal displacement of each dot is proportional to the resulted deflection angle over a subaperture; the deflection angle is in turn a local gradient of Optical Path Difference or OPD. As OPD is proportional to the spanwise-integrated density field,  $OPD(x, y, t) = K_{GD} \int \rho'(x, y, z, t) dz$  [26], where  $K_{GD}$  is the Gladstone-Dale constant, time series of the deflection angle carry information about the temporal evolution of the density field over a subaperture. It is important to note that aero-optical measurements are non-intrusive by nature, sensitive to the density field only, and limited in temporal resolution only by the digital camera technology.

The same optical setup was also used to collect high-speed shadowgraph movies. To do this, the lenslet array was removed and distorted intensity patterns were recorded at the same sampling speed over the same 64x128 area. The representative shadowgraph image with overlaid dot pattern is shown in Fig. 7. Several flow regions, indicated by yellow circles in Fig. 7, were selected to investigate the temporal dynamics and the sensitivity to the plasma generators: point BL2 is inside the separated bubble, A2 and A3 correspond to the unsteady shock over the separation bubble, and A4 is in the outside portion of the flow downstream of the plasma generators. In-house software was used to extract the temporal motion of the dots and to convert this into a time series of the deflection angles.

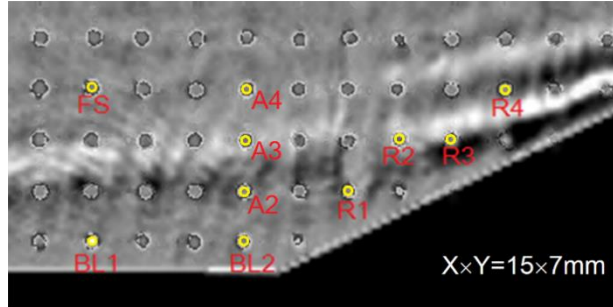


Fig. 7. Shadowgraph image with overlaid dot pattern to identify different flow regions near the model corner.

## V. Tests Results

Test 1 consisted of a visualization of gas disturbances appearing at the SCD generation in stagnant (no flow) air at atmospheric pressure and at decreased pressure equal to that in high-speed flow,  $P = 4 - 10 \text{ mBar}$ . The shock wave travelling outward from the model surface and a thermal distortion are observed as a result of plasma generation as it is shown in Fig. 8. It demonstrates a pointwise excitation of the gas distortion due to the SCD operation.

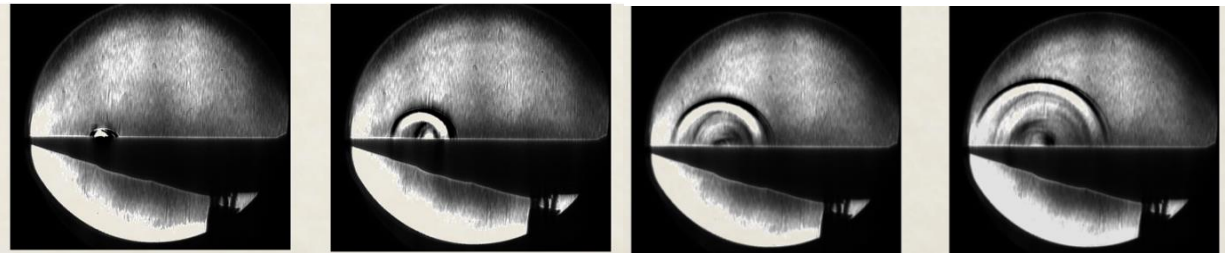


Fig.8. SCD in stagnant air,  $P=1\text{Bar}$ . Gas perturbation taken by schlieren system, exposure  $t=0.1\mu\text{s}$ , delay time  $t= 5, 25, 45, 75\mu\text{s}$  (from left to right).

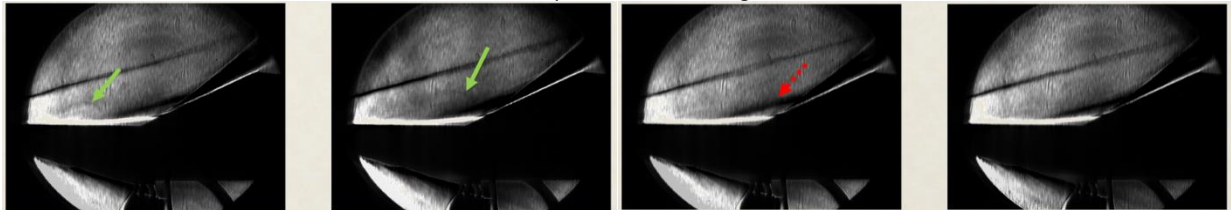


Fig.9. SCD in flow  $M=4.5$  flow at delays 20, 40, 60, 80  $\mu\text{s}$  after plasma pulse. Boundary layer, corner separation bubble, and related shocks are well-visualized. Shock wave front (due to plasma) is indicated by green arrows. Position of separation zone related shock wave (red dashed arrow) is affected by plasma distortion: being pushed down then return back.

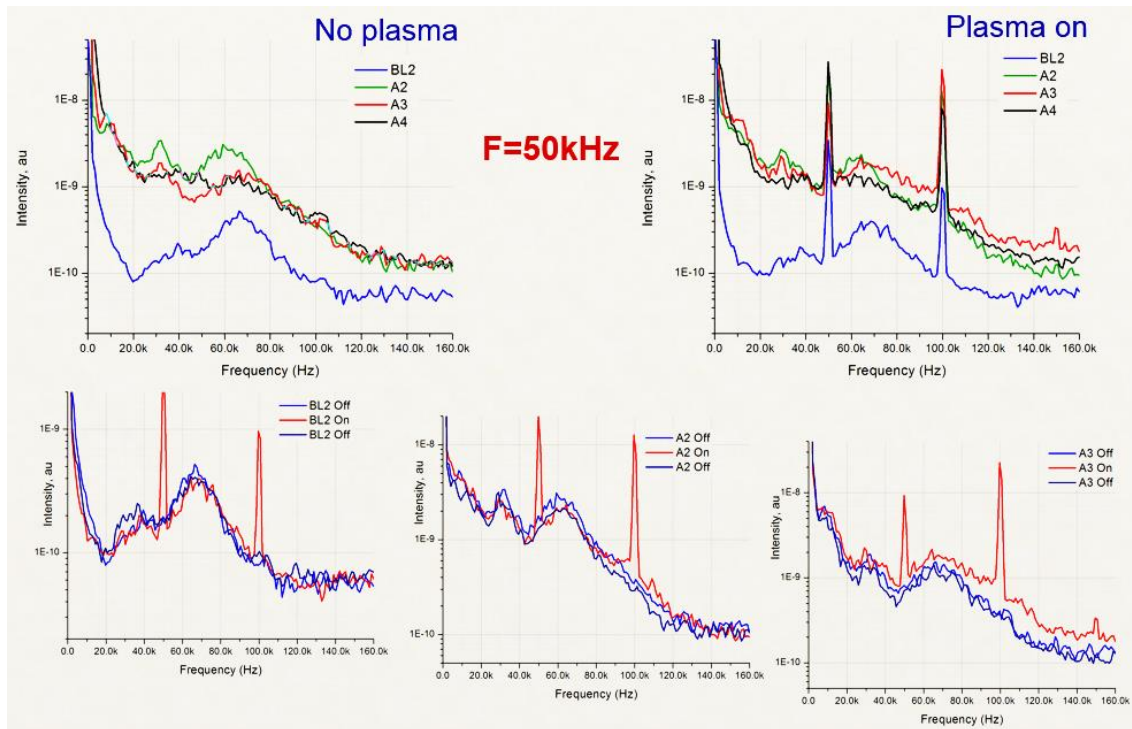
During Test 2 the plasma effect and its resulting generation of an outgoing shock wave and a thermal bubble travelling along the top surface of the model were studied, as shown in the schlieren images in Fig. 9. Finally the

plasma-based perturbation delivers the extra momentum to the BL that may lead to an earlier laminar-turbulent transition and to prevent a separation on the compression ramp. Those two tests deliver the data to formulate intermediate conclusions: (1) even a single pulse affects the flow structure; and (2) optical methods are appropriate for diagnostics of weak flow disturbances, which are typical for this study.

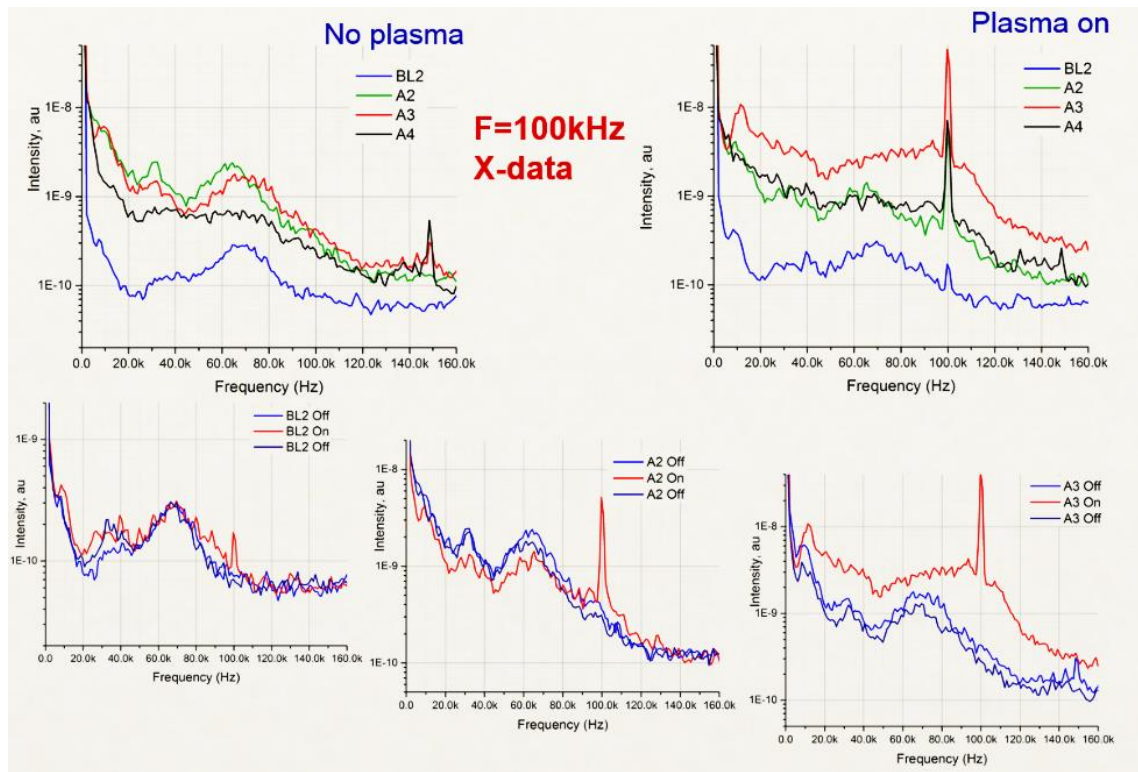
Test 3 was dedicated to the study of a pulse-repetitive plasma effect on the spectrum of flow perturbations. The aero-optical technique with the high-speed wavefront sensor has been applied to acquire the data. After a series of preliminary measurements it was found that the plasma generation affects the spectrum only slightly if the repetition frequency is less than the dominant frequency of the first-mode instability,  $F_1 = 60 - 80 \text{ kHz}$ . For a plasma frequency greater than  $F_1$ , the plasma effect is significant. Figures 10a and 10b show data for plasma actuation frequencies of 50 and 100 kHz, respectively. Every test's measurements included 0.1 s of spectrum analysis prior to plasma actuation, 0.1 s with plasma operation, and 0.1 s after the plasma has turned off (to ensure there was no shift of flow parameters during operation).

At  $f = 50 \text{ kHz}$ , the plasma effect is really small in most areas (Fig. 10a). Some effect is visible in the shear layer (point A3, see Fig. 7 for a reference). Amplitudes of high-frequency disturbances ( $> 80 \text{ kHz}$ ) appear to increase. At the plasma repetition frequency  $f = 100 \text{ kHz}$  (Fig. 10b and 10c), the plasma effects were observed at all points except A4, the “free stream” conditions.

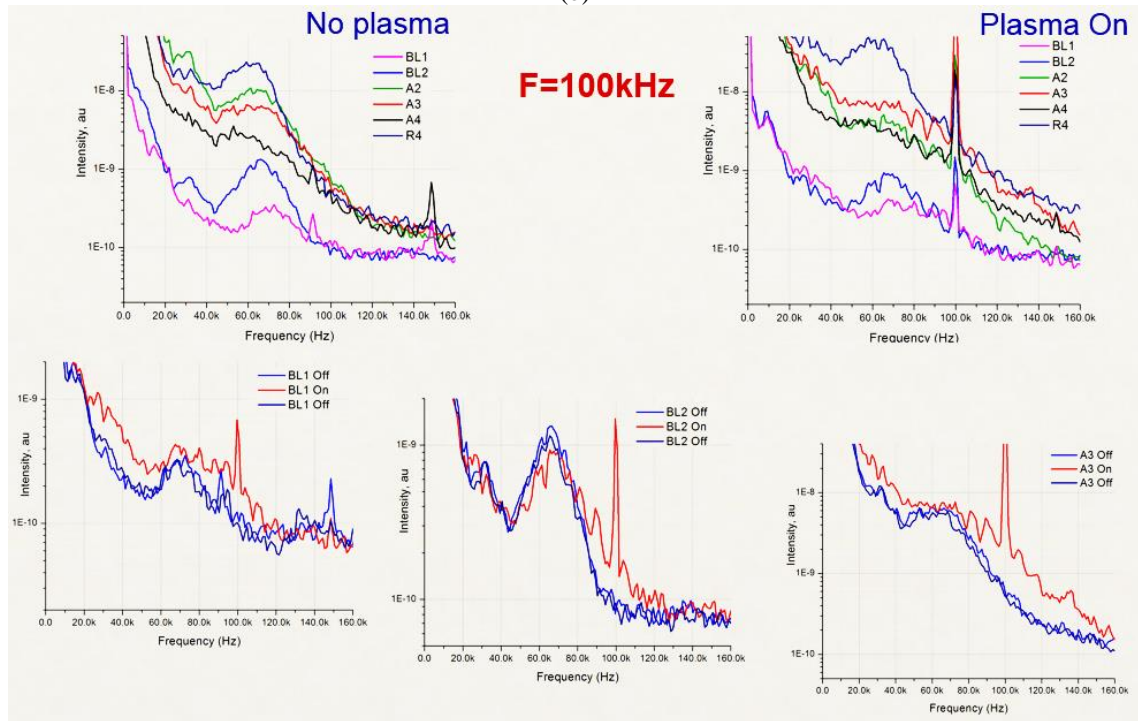
The wavefront sensor measures both, X and Y, components of the wavefront gradient or, equivalently, the deflection angle. This is in contrast to the Schlieren technique, where wavefront changes along only one fixed direction are measured. In isotropic flows both components are typically of the same magnitude, while for the current flow of interest the wall-normal, Y-component of the deflection angle is expected to be larger, compared to the streamwise, X-component, due to higher density gradients in the wall-normal direction. The comparison of Fig.10b and Fig.10c shows a significantly higher values of the flow disturbances measured in the wall-normal Y-direction vs ones in the longitudinal X-direction. The effect of the plasma generation, reflected in the increasing of a spectral density of flow disturbances, has a bigger magnitude as well (note, the Y-scale is logarithmic).



(a)



(b)



(c)

Fig. 10. Spectra of flow disturbances. a. – X-component, plasma excitation  $f = 50 \text{ kHz}$ ; b. – X-component, plasma excitation  $f = 100 \text{ kHz}$ ; Y-component, plasma excitation  $f = 100 \text{ kHz}$ . (Fig.7 for reference)



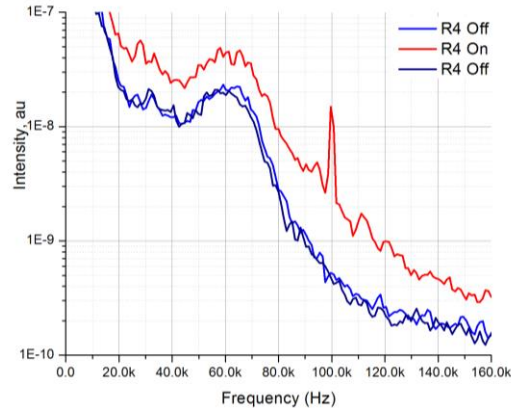


Fig. 11. Spectra of flow disturbances on the ramp, point R4 (Fig.7 for reference).

Amongst the points observed in this test the maximal effect of the plasma was detected for the flow on the ramp, point R4 in Fig. 7, close to a root part of the ramp-related shock, as it is shown in Fig. 11. It results in an amplification of the amplitude of gas perturbations,  $A/A_0 = 2 - 8$ , in a wide range of spectra including high-frequency oscillations  $f > 100 \text{ kHz}$ .

## VI. Summary

The current results of the study of a transient electrical discharge application for the control of the boundary layer transition in high-speed flow are summarized below.

1. Analysis of the plasma-based boundary layer transition control at high-speed external flow shows a range of parameters, where artificial disturbances generated by electrical discharge may provoke the transition. Basic consideration includes the periodic arrangement of the multi-element plasma array on the model surface. The frequency of disturbances has to be adjusted to the flow velocity.

2. One of the most important problems appears in the generation of a contracted plasma within a low density gas, which is typical for a hypersonic boundary layer. The shallow cavity discharge (SCD) was shown to be quite appropriate with the objective of the work.

3. The draft design of the plasma-based actuator for high-speed transition control is proposed. It consists of a 1D array of SCD plasma elements and a power supply with individual control of each discharge cell. In addition to the scientific results obtained, the third test series was performed to check the operational limits of the electrode system and prove the feasibility of power supply operation at high repetition frequencies. This was successful in proving the operational capabilities of the setup used for frequencies up to  $100 \text{ kHz}$ .

4. Tests demonstrate:

- the receptivity of hypersonic BLs to highly transient plasmas;
- the feasibility of hypersonic BL active tripping by electric discharges with a frequency of oscillations  $f > F_1$  ;
- a high potential of aero-optical techniques to perform non-intrusive, high-frequency (up to  $1 \text{ MHz}$ ), spatially-resolved measurements of flow structure and dynamics.

### Acknowledgement

The current work is supported by the FlowPAC Institute at the University of Notre Dame. A portion of this work (design of the SCD plasma actuator [22]) was previously supported by MBDA-France (Mr. Francois Falempin supervision).

### References

1. A. Valdivia, K. B. Yuceil, J. L. Wagner, N. T. Clemens, and D. S. Dolling, "Control of Supersonic Inlet-Isolator Unstart Using Active and Passive Vortex Generators", *AIAA Journal*, June, Vol. 52, No. 6 : pp. 1207-1218
2. Yu Wu • Shihe Yi • Lin He • Zhi Chen • Yangzhu Zhu, "Flow visualization of Mach 3 compression ramp with different upstream boundary layers", *J Vis* (2015) 18:631-644
3. Berry, S. A., Nowak, R. J., and Horvath, T. J., "Boundary Layer Control for Hypersonic Airbreathing Vehicles," AIAA-2004-2246, 28 June - 1 July, 2004, Portland, Oregon.

4. Schneider, S.P., "Effects of Roughness on Hypersonic Boundary-Layer Transition," *J. of Spacecraft and Rockets*, Vol. 45, No. 2, pp. 193–209, March-April 2008.
5. Reshotko, E., and Tumin, A., "Role of Transient Growth in Roughness-Induced Transition," *AIAA J.*, Vol. 42, No. 4, pp. 766–770, April 2004.
6. Choudhari, M., Li, F., and Edwards, J., "Stability Analysis of Roughness Array Wake in a High-Speed Boundary Layer," *AIAA-2009-170*, 5 - 8 January 2009, Orlando, Florida.
7. Yan, H., and Gaitonde, D., "Effect of Thermally Induced Perturbation in Supersonic Boundary Layers," *Physics of Fluids*, Vol. 22, 2010, 064101(1-17).
8. Adamovich, I.V., Little, J., Nishihara, M., Takashima, K., and Samimy, M., "Nanosecond Pulse Surface Discharges for High-Speed Flow Control", *AIAA Paper 2012-3137*, 6th AIAA Flow Control Conference, 25-28 June 2012, New Orleans, LA
9. Corke, T.C., Enloe, C.L., and Wilkinson, S.P., "Dielectric Barrier Discharge Plasma Actuators for Flow Control", *Annual Review of Fluid Mechanics*, vol. 42, 2010, pp. 505-529
10. Kotsonis, M, Correale, G, Michelis T, Ragni D, Scarano F, "Nanosecond-pulsed plasma actuation in quiescent air and laminar boundary layer", *Journal of Physics D: Applied Physics* 47 (10), 2014, 105201
11. Kriegseis, J., Duchmann, A., Tropea, C., and Grundmann, S., "On the classification of dielectric barrier discharge plasma actuators: A comprehensive performance evaluation study", *Journal of Applied Physics*, vol. 114, 2013, p. 053301
12. Leonov, S., Opaitis, D., Miles, R., Soloviev, V., "Time-Resolved Measurements of Plasma-Induced Momentum in Air and Nitrogen under DBD Actuation", *PHYSICS OF PLASMAS* 17, 113505, 6 (Oct), 2010
13. Moreau, E., "Airflow Control by Non-thermal Plasma Actuators", *Journal of Physics D: Applied Physics*, vol. 40, No.3, 2007, pp. 605-636
14. Macheret, S.O., Shneider, M.N. and Miles, R.B., "Magneto hydrodynamic and Electrohydrodynamic Control of Hypersonic Flows of Weakly Ionized Plasmas," *AIAA J.*, Vol.42, No.7, 2004, pp. 1378-1387.
15. Meyer, R., Palm, P., Ploenjes, E., Rich, J.W., and Adamovich, I.V., "The Effect of a Nonequilibrium RF Discharge Plasma on a Conical Shock Wave in a M=2.5 Flow," *AIAA J.*, Vol. 41, No. 5, 2003, pp. 465-469.
16. Minucci, M.A.S., Toro, P.G.P., Oliveira, A.C., Ramos, A.G., Chanes, J.B., Pereira, A.L., Nagamatsu, H.T., Leik, and Myrabo, N., "Laser-Supported Directed-Energy "Air Spike" in Hypersonic Flow," *Journal of Spacecraft and Rockets*, Vol.42, No.1, 2005, pp. 51-57.
17. Leonov, S., Yarantsev, D., Kuryachii, A., and Yuriev, A., "Study of Friction and Separation Control by Surface Plasma," *AIAA-2004-512*, 5-8 January, Reno, Nevada.
18. Adelgren, R.G., Elliott, G.S., Crawford, J.B., Carter, C.D., Donbar, J.M., and Grosjean, D.F., "Axisymmetric Jet Shear-Layer Excitation Induced by Laser Energy and Electric Arc Discharges," *AIAA J.*, Vol.43, No. 4, 2005, pp. 776-791.
19. Samimy, M., Adamovich, I., Webb, B., Kastner, J., Hileman, J., Keshav, S., and Palm, P., "Development and Characterization of Plasma Actuators for High Speed Jet Control," *Experiments in Fluids*, Vol. 37, No. 4, 2004, pp. 577-588.
20. Francois Falempin, Alexander A. Firsov, Dmitry A. Yarantsev, Marat A. Goldfeld, Konstantin Timofeev, Sergey B. Leonov, "Plasma Control of Shock Wave Configuration in Off-Design Mode of M=2 Inlet", *Experiments in Fluids*, March 2015, DOI: 10.1007/s00348-015-1928-4
21. Leslie M. MACK. "Linear Stability Theory and the Problem of Supersonic Boundary- Layer Transition", *AIAA Journal*, Vol. 13, No. 3 (1975), pp. 278-289.
22. Sergey B. Leonov, Alec Houpt, Francois H. Falempin, "Control of Hypersonic BL Transition by Electrical Discharge (feasibility study)", *AIAA 2015-3602*, 20th AIAA International Space Planes and Hypersonic Systems and Technologies Conference, 2015, 10.2514/6.2015-3602
23. Raizer Yu P 1991 *Gas Discharge Physics* (Berlin: Springer)
24. Tyson RK. 1997. *Principles of Adaptive Optics*. New York: Academic. 345 pp. 2th ed.
25. Sontag, J. and Gordeyev, S., " Non-intrusive Velocity and Density Measurements in Subsonic Turbulent Boundary Layer ", *AIAA Paper 2015-3247*, 2015.
26. Wang, M., Mani, A. and Gordeyev, S. "Physics and Computation of Aero-Optics", *Annual Review of Fluid Mechanics*, Vol. 44, 2012, pp. 299-321.